MNRAS **000**, 1–4 (2015) Preprint 3 September 2018 Compiled using MNRAS LATEX style file v3.0

EAGLE GALAXIES IN VOIDS

XXX,[1⋆] A. N. Other,[2] Third Author[2,3] and Fourth Author[3]
[1]*Royal Astronomical Society, Burlington House, Piccadilly, London W1J 0BQ, UK*
[2]*Department, Institution, Street Address, City Postal Code, Country*
[3]*Another Department, Different Institution, Street Address, City Postal Code, Country*

Accepted XXX. Received YYY; in original form ZZZ

ABSTRACT

XXXXXXXXX

Key words: keyword1 – keyword2 – keyword3

1 INTRODUCTION

To be editted

2 METHODOLOGY

2.1 Simulations

We use the largest simulation from the EAGLE project (Schaye et al. 2015; Crain et al. 2015) [1] that comprises several cosmological simulations in which varies the galaxy formation sub-grid models, numerical resolutions and volumes. The simulations were performed with the modified version of SPH code P-Gadget 3 that is an improved version of Gadget 2 (Springel 2005b) and includes galaxy formation sub-grid models to capture unresolved physics including cooling, metal enrichment and energy input from star formation and black hole growth. A full description of EAGLE is found in Schaye et al 15 and Crain et al 15. Here, we concentrate on the largest simulation in EAGLE with the reference galaxy formation model and is denoted as Ref-L100N1504with a comoving volume of $(100\mathrm{cMpc})^3$. A mass resolution of $9.7\times10^6\mathrm{M}_\odot$ for dark matter (and $1.81\times10^6\mathrm{M}_\odot$ for baryonic) particles and a softening length of 2.66ckpc [2] limited to a maximum physical size of 0.70pkpc . The simulation adopts the Λ-CDM cosmological with parameters taken from the Planck Collaboration et al. 2014.

The simulation outputs were analysed using the SUBFIND programme to identify bound sub-structures (Springel et al. 2001; Dolag et al. 2009) within each dark matter halo. We identify these substructures as galaxies and measure stellar masses within a radius of 30 pkpc.

⋆ E-mail: mn@ras.org.uk (KTS)
[1] http://eaglesim.org
http://eagle.strw.leidenuniv.nl
[2] we will refer to comoving distances by preceding a 'c' such as ckpc to refer to comoving kiloparsec and physical lengths will be preceded by a ' p' as pkpc

3 VOID CATALOGUE IN EAGLE

3.1 Description

We use the void catalogue of Paillas et al 2017 in EAGLE. To define a void is ....

4 GALAXY SAMPLE

We use galaxies whose stellar mass is higher than $10^9\mathrm{M}_\odot$. For each galaxy, we calculate their distance to the centre of all voids and only associate it wiht the void whose centre has the minimum distance to the given galaxy. In this way one galaxy is associated to one void. To determine the environmental effects of the large structure on the galaxies in EAGLE, we split into 4 samples depending on the distance to the centre of the associated void. The first sample, namely 'inner void', are galaxies with distances r to the centre of their associated void between 0 and $0.8r_{\mathrm{void}}$, where r_{void} is the radius of the void. The second sample, namely 'outer void', comprises galaxies with distances $0.8 \leq r/r_{\mathrm{void}} < 1$, the third sample, namely boundary ,are formed by galaxies between the boundary of the voids and the filaments and with distances are such that $1 \leq r/r_{\mathrm{void}} < 1.2$, and the fourth sample, namely filaments, are formed by the rest of the galaxies and whose distances are larger than $r/r_{\mathrm{void}} \geq 1.2$ and are galaxies located in filaments.

The left panel of Fig. 1 shows the star mass distribution of the four samples. Note that the star mass distribution in the inner void sample (blue colour) is dominated for small galaxies in comparison to the rest of the samples whose fraction of galaxies smaller than $10^{10}\mathrm{M}_\odot$ decreases gradually as the distance of the centre of the void is higher. To disentangle the dependence of the stellar mass in our samples, we use a subsamples such that the same stellar mass distribution match with that of the inner void sample as is shown in the right panel of Fig. 1. We also show a visualisation of the position of the galaxies in the simulation in Fig 2. To give a sense of the number of galaxies used, we account for 513 in the inner void sample, 588 in the outer void sample , 3932 and 8167 galaxies in the boundary sample and the filament sample respectively.

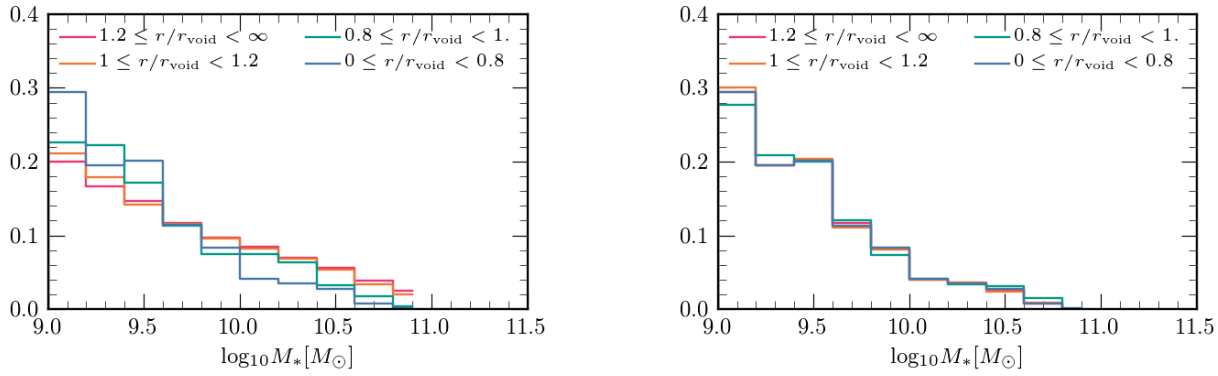

Figure 1. *Left panel*: The stellar mass distribution of the four galaxies samples defined as a function the distance to the centre of the closest void as the legend indicates. The inner void sample is more dominated by low mass galaxies in comparison to the rest of the other galaxy samples. *Right panel*: The stellar mass distribution of a subsample of each galaxy sample matching the same stellar mass distribution as the inner void sample

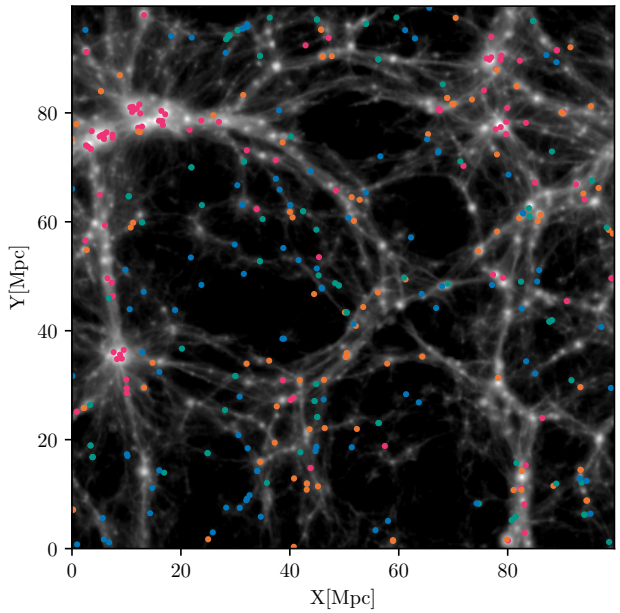

Figure 2. A slice of $100 \times 100 \times 25$cMpc of the galaxies in the simulation Ref-L100N1504at $z = 0$. Coloured circles represent a different galaxies sample as the legend specifies.

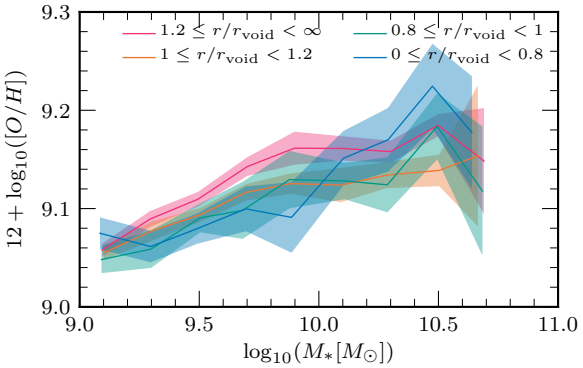

Figure 3. *Left panel*: The median stellar mass-Oxygen abundances relation using star forming gas in galaxies for the Ref-L100N1504 simulation for each galaxy sample. The filled regions represent the errors of the medians via bootstrapping technique. No difference is found between samples.

5 RESULTS

Here, we describe the results of the properties of galaxies in voids.

We look at the merger history of the galaxies in the inner parts and outer parts of the voids. We find that galaxies that have at least one merger with a mass ratio ≥ 0.1 is 10.4% in the inner part and 9.7% in the outer part of the voids, showing no significant difference.

We also find a small number of galaxies with a disc in order to calculate the metallicity gradients.

We are planning to calculate a global metallicity gradient without including the bulge to disc decomposition.

6 SUMMARY AND DISCUSSION

ACKNOWLEDGEMENTS

The Acknowledgements section is not numbered. Here you can thank helpful colleagues, acknowledge funding agencies, telescopes and facilities used etc. Try to keep it short.

REFERENCES

Abramowicz, M. A. , Chen, X. , Taam, R. E., 1995, ApJ, 452, 379.
Aird, J. , Nandra, K. , Laird, E. S. and Georgakakis, A. , Ashby, M. L. N. , Barmby, P. , Coil, A. L. , Huang, J.-S. , Koekemoer, A. M. , Steidel, C. C. and Willmer, C. N. A. 2010, MNRAS, 401, 2531.
Aird, J., Coil, A. L., Georgakakis, A., et al. 2015, arXiv:1503.01120
Anglés-Alcázar, D., Davé, R., Faucher-Giguère, C.-A., Özel, F., & Hopkins, P. F,, 2016, arXiv:1603.08007
Bahé, Y. M., Crain, R. A., Kauffmann, G., et al. 2016, MNRAS, 456, 1115
Bandara, K., Crampton, D., Simard, L., 2009, ApJ, 704, 1135.
Binney J., Tabor G., 1995, MNRAS, 276, 663.

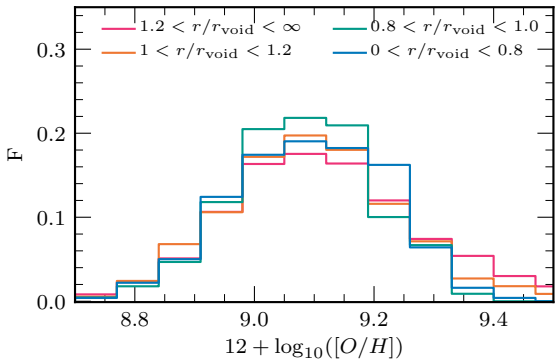

Figure 4. The oxygen abundance distribution of the galaxy star forming regions. Each colour represents different galaxy sample as the legend indicates. Visually, there is a weak tendency in the void sample to have a higher fraction with higher values of O/H than the rest of the samples. Performing the Kolmogorov-Smirnov test between the inner void sample (blue) and filament sample (magenta), we found a p-value of 3.6×10^{-36}, confirming that there is negligible probability that the distribution of the two sample are drawn for the same population.

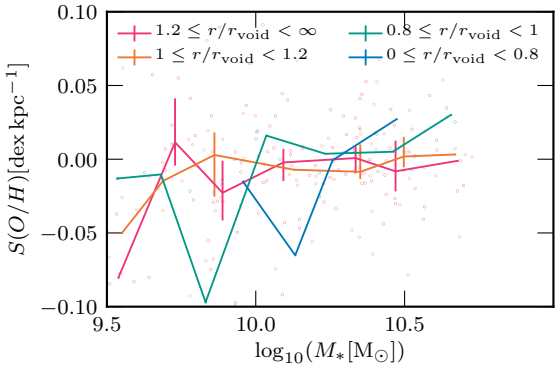

Figure 5. The metallicity gradients as a function of stellar mass.

Bondi H., Hoyle F., 1944, MNRAS, 104, 273.
Booth C. M., Schaye J., 2009, MNRAS, 398, 53.
Booth C. M., Schaye J., 2010, MNRAS, 405, L1.
Bower R. G., Benson A. J., Malbon R., Helly J. C., Frenk C. S., Baugh C. M., Cole S., Lacey C. G., 2006, MNRAS, 370, 645.
Buchner J., Georgakakis A., Nandra K., et al. 2015, ApJ, 802, 89.
Chabrier, G., 2003, PASP, 115, 763.
Choi, E., Naab, T., Ostriker, J. P., Johansson, P. H., & Moster, B. P., 2014, MNRAS, 442, 440.
Churazov E., Brüggen M., Kaiser C. R., Böhringer H., Forman W., 2001, ApJ, 554, 261.
Comerford, J. M., & Greene, J. E. 2014, ApJ, 789, 112
Comerford, J. M., Pooley, D., Barrows, R. S., et al. 2015, ApJ, 806, 219
Crain R. A., Theuns T., Dalla Vecchia C., Eke V. R. , Frenk S. C., Jenkins A., Kay S. T. and Peacock J. A. *et al.*, 2009, MNRAS, 399, 1773.
Crain, R. A., Schaye, J., Bower, R. G., et al. 2015, arXiv:1501.01311
Croton D. J., Springel V., White S. D. M., De Lucia G., Frenk S. C., Gao L., Jenkins A. and Kauffmann G. *et al.*, 2006, MNRAS, 365, 11.
Cullen, L. and Dehnen, W., 2010, MNRAS, 408, 669.
Dalla Vecchia C. and Schaye J., 2012, MNRAS, 426, 140.
De Lucia G., Blaizot J., 2007, MNRAS, 375, 2
Di Matteo, T. and Colberg, J. and Springel, V. and Hernquist, L. and Sijacki, D., 2008, ApJ, 676, 33.
Done, C., Gierliński, M., & Kubota, A. 2007, A&ARv, 15, 1
Durier, F. and Vecchia D. C., 2012, MNRAS, 419, 465.
Fanidakis N. and Baugh C. M. and Benson A. J. and Bower R. G. and Cole S. and Done C. and Frenk C. S. and Hickox R. C. and Lacey C. and Del P. Lagos C., 2012, MNRAS, 419, 2797.
G. J. Ferland, R. L. Porter, P. A. M. van Hoof, R. J. R. Williams, N. P. Abel, M. L. Lykins, Gargi Shaw, W. J. Henney, and P. C. Stancil, 2013, Rev. Mex. Soc., 49, 1.
Furlong, M., Bower, R. G., Theuns, T., et al. 2015, MNRAS, 450, 4486
Furlong, M., Bower, R. G., Crain, R. A., et al. 2015, arXiv:1510.05645
Giallongo, E., Grazian, A., Fiore, F., et al., 2015, AAP, 578, A83
Graham, A. W., 2016, Galactic Bulges, 418, 263
Grogin, N. A., Kocevski, D., Faber, S. et al. 2011, ApJS, 197, 37
Haardt, F. and Madau, P., 2001, Clusters of Galaxies and the High Redshift Universe Observed in X-rays, astro-ph/0106018.
Hasinger, G. and Miyaji, T. and Schmidt, M., 2005, A&A, 441, 417.
Hasinger, G., 2008, A& A, 490, 905.
Hirschmann, M., Dolag, K., Saro, A., et al. 2014, MNRAS, 442, 2304
Hirschmann M., Somerville R. S., Naab T., Burkert A., 2012, MNRAS, 426, 237
Hopkins, P. F., Richards, G. T., & Hernquist, L., 2007, ApJ, 654, 731
Hopkins P. F., and Hernquist L., Cox T. J. , Keres D. and Wuyts S., 2009, ApJ, 691, 1424.
Jenkins A., 2010, MNRAS, 403, 1859.
Jenkins A., 2013, MNRAS, 434, 2094.
Kelly B. C., Shen Y., 2013, ApJ, 764, 45.
Kennicutt, Jr., R. C., 1998, ARA&A, 36, 189.
Khandai, N. and Di Matteo, T. and Croft, R. and Wilkins, S. M. and Feng, Y. and Tucker, E. and DeGraf, C. and Liu, M.-S., 2015, MNRAS, 450, 1349
Koekemoer, A. M., Faber, S., Ferguson, H. et al. 2011, ApJS, 197, 36
Kormendy, J. and Ho, L. C., 2013, ARA&A ,51,511.
Koss, M., Mushotzky, R., Treister, E., et al. 2012, ApJl, 746, L22
Lagos, C. d. P., Crain, R. A., Schaye, J., et al., 2015, arXiv:1503.04807
Lansbury, G. B., Gandhi, P., Alexander, D. M., et al., 2015, ApJ, 809, 115
Lewis A., Challinor A., Lasenby A., 2000, ApJ, 538, 473
Liu, X., Shen, Y., Strauss, M. A., & Hao, L. 2011, ApJ, 737, 101
Lusso, E., Comastri, A., Simmons, B. D., et al., 2012, MNRAS, 425, 623
Madau, P., & Haardt, F., 2015, ApJ, 813, L8
Marconi, A. and Risaliti, G. and Gilli, R. and Hunt, L. K. and Maiolino, R. and Salvati, M., 2004, MNRAS, 351, 169.
McAlpine S., Helly J.C., Schaller M., et al. 2015, arXiv:1510.01320
McCarthy I. G., Schaye J., Ponman T. J., Bower R. G., Booth C. M., Dalla Vecchia C., Crain R. A. and Springel V., 2010, MNRAS, 406, 822.
McConnell, N. J., & Ma, C.-P., 2013, ApJ, 764, 184
Miyaji T., Hasinger G., Schmidt M., 2000, A&A, 353, 25.
Miyaji, T., Hasinger, G., Salvato, M., et al., 2015, ApJ, 804, 104
Narayan, R. and Yi, I., 1994, ApJ, 428, L13.
Planck Collaboration and Ade, P. A. R. and Aghanim, N. and Alves, M. I. R. and Armitage-Caplan, C. and Arnaud, M. and Ashdown, M. and Atrio-Barandela, F. and Aumont, J. and Aussel, H. and et al., 2013, arxiv e-prints, 1303.5062.
Portinari L., Chiosi C., & Bressan A. 1998, A& A, 334, 505.
Power, C. and Nayakshin, S. and King, A., 2011, MNRAS, 412, 269.
Rees, M. J. and Begelman, M. C. and Blandford, R. D. and Phinney, E. S., 1982, NATURE, 295, 17.
Rosas-Guevara Y. M., Bower R.G., Schaye J., et al. 2015, MNRAS, 454, 1038
Rosas-Guevara, Y., Bower, R. G., Schaye, J., et al. 2016, MNRAS, 462, 190
Shakura N.I ., Syunyaev R. A., 1973, A&A , 24, 337.
Schaller, M., Dalla Vecchia, C., Schaye, J., et al., 2015, MNRAS, 454, 2277
Schaye, J., 2004, ApJ, 609, 667
Schaye J., Dalla Vechia C., 2008, MNRAS, 383, 1210.
Schaye J., Dalla Vecchia C., Booth C. M., Wiersma R. P. C., Theuns T.,

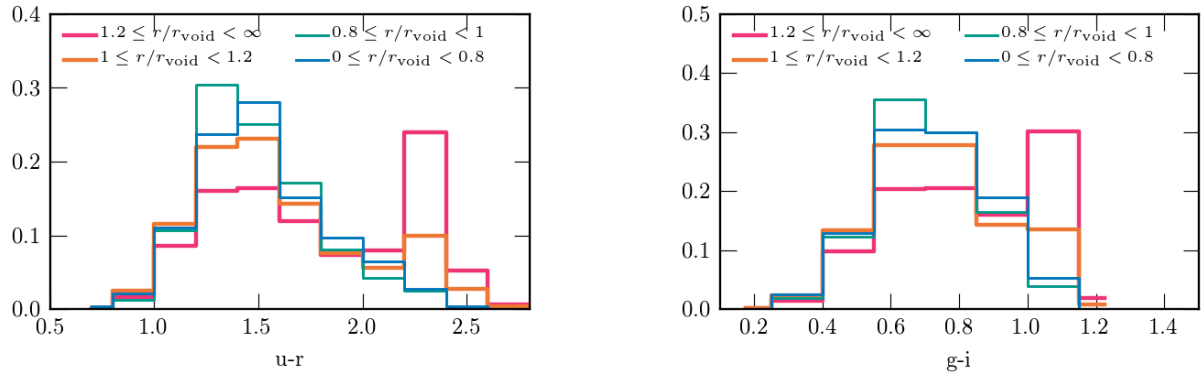

Figure 6. *Left panel:* The fraction distribution of galaxies as a function of $u-r$ for the different galaxy samples. *Right panel*: The same plot as the Left panel but as a function of $g-i$. In both panels, it is shown a different shape of the distribution for different galaxy samples. For inner void and outer void samples there is one peak distribution centred on 'bluer' galaxies while the filament and boundary samples the distribution shows a double peak where the second peak is located in 'redder galaxies'. Performing the Kolmogorov-Smirnov test between the inner void sample (blue) and filament sample (magenta), we found p-values of 3.0×10^{-33} and 2.4×10^{-32} for the distribution in $u-r$ and $g-i$ respectively.

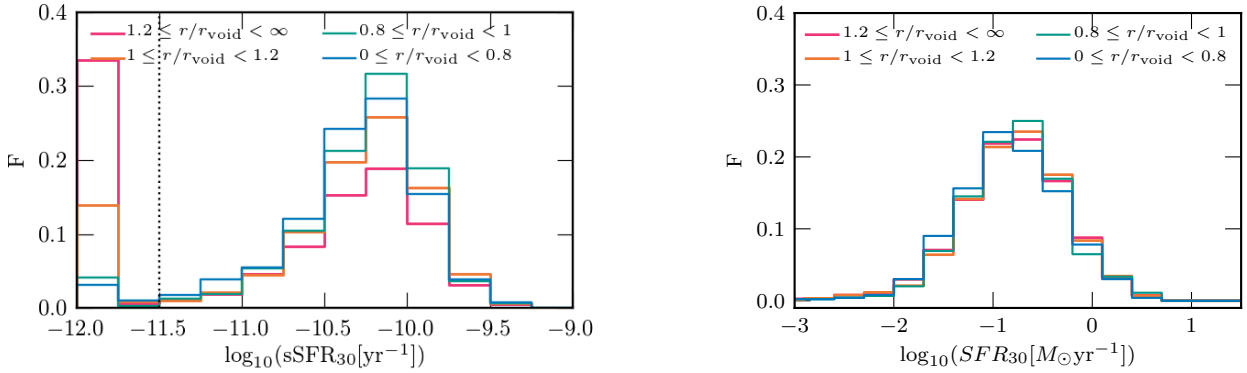

Figure 7. *Left panel:* The distribution of the sSFR in a 30-kpc-aperture, sSFR_{30},. The galaxies with $\mathrm{sSFR}_{30} < 10^{12} \mathrm{M}_\odot \mathrm{yr}^{-1}$ are set with a value $10^{-12.5}$, to show the fraction of non active galaxies (left region of the dotted line) in each galaxy sample. The plot shows that there is a higher fraction of active galaxies in the inner void and outer void samples in comparison to the other samples. In the filament sample, there is a higher fraction of non active galaxies ($> 30\%$) than the inner void sample which there is less than 5%. *Right panel:* The distribution of the SFR for the different galaxy samples. Performing a KS test we find p-values of 8.63×10^{-40}, rejecting the hypothesis that they are similar populations.

Haas M. R., Bertone S. and Duffy A. R.*et al.*, 2010, MNRAS, 402, 1536.
Schaye, J., Crain, R. A., Bower, R. G., et al. 2015, MNRAS, 446, 521
Schmidt, M., 1959, ApJ, 129, 243.
Shankar, F. and Salucci, P. and Granato, G. L. and De Zotti, G. and Danese, L., 2004, MNRAS, 354, 1020.
Shankar, F., 2013, Classical and Quantum Gravity, 30, 244001
Sijacki D., Springel V., Di Matteo T. and Hernquist L., 2007 MNRAS, 380, 877.
Sijacki, D., Vogelsberger, M., Genel, S., et al. 2015, MNRAS, 452, 575
Soltan A., 1982, MNRAS, 200, 115.
Springel V., Di Matteo T. and Hernquist L., 2005, MNRAS, 361, 776.
Springel, V., 2005b, MNRAS, 364, 1105.
Steffen, A. T. and Barger, A. J. and Cowie, L. L. and Mushotzky, R. F. and Yang, Y., 2003, ApJ, 596, L23.
Steinborn, L. K., Dolag, K., Comerford, J. M., et al. 2016, MNRAS, 458, 1013
Trayford, J. W., Theuns, T., Bower, R. G., et al. 2016, arXiv:1601.07907
Tremaine S., Gebhardt K., Bender R., Bower G., Dressler A., Faber S. M., Filippenko A. V. and Green R. *et al.*, 2002, ApJ, 574, 740.
Treister, E., Urry, C. M., & Virani, S., 2009, ApJ, 696, 110
Ueda, Y. and Akiyama, M. and Ohta, K. and Miyaji, T., 2003,ApJ , 598, 886.
Ueda, Y., Akiyama, M., Hasinger, G., Miyaji, T., & Watson, M. G. 2014, ApJ, 786, 104
Vasudevan R. V., Fabian A. C., 2009, MNRAS, 392, 1124
Vogelsberger, M., Genel, S., Springel, V., et al., 2014, MNRAS, 444, 1518
Volonteri, M., Dubois, Y., Pichon, C., & Devriendt, J. 2016, MNRAS, 460, 2979
Yu, Q. and Tremaine, S., 2002, MNRAS, 335, 965.
Wiersma R. P. C., Schaye J., Theuns T., Smith B. D, 2009, MNRAS, 393, 99.
Wiersma R. P. C., Schaye J., Theuns T., Dalla Vecchia C. and Tornatore L., 2009, MNRAS, 399, 574.

This paper has been typeset from a TEX/LATEX file prepared by the author.

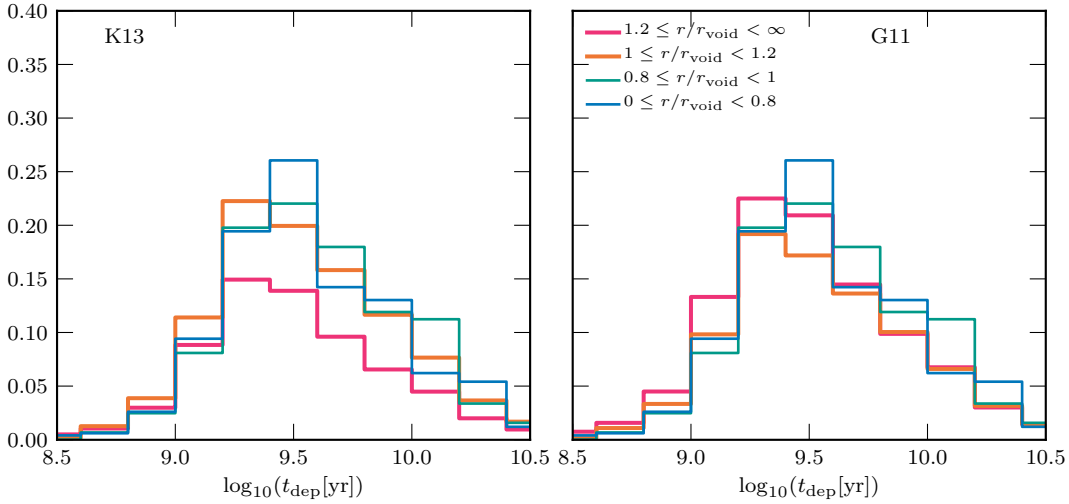

Figure 8. Distributions of the depletion times using the HI and H2 gas mass estimated by Lagos et al. (2015). Galaxies in the inner void (blue lines) and outer void samples (green lines) tend to have longer depletion times in comparison to the galaxies in the boundary (orange) and filament (magenta) samples. The distribution of the inner void sample and the filament sample are different with a KS p-value of 1.62×10^{-43}.

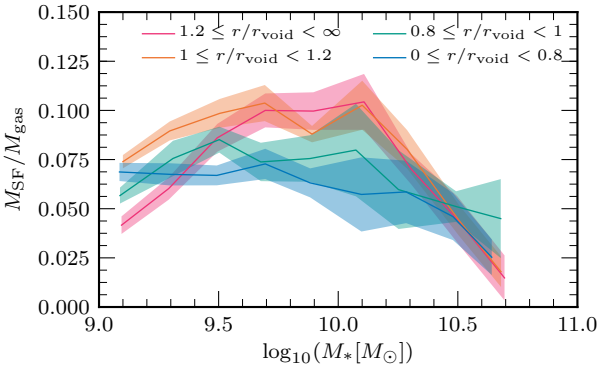

Figure 9. Star formation efficiency as a function of stellar mass

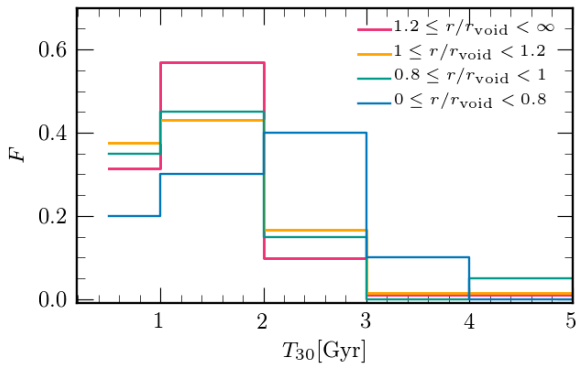

Figure 10. The age distribution of the youngest 30 percent of the stars for central disc galaxies in each sample. Galaxies in the inner void sample tend to have older stars than the other samples. We calculate the KS p-value for each distribution against the inner void sample and we did not find any statistically significant difference at a probability of 5% or lower between the inner void and the other samples.

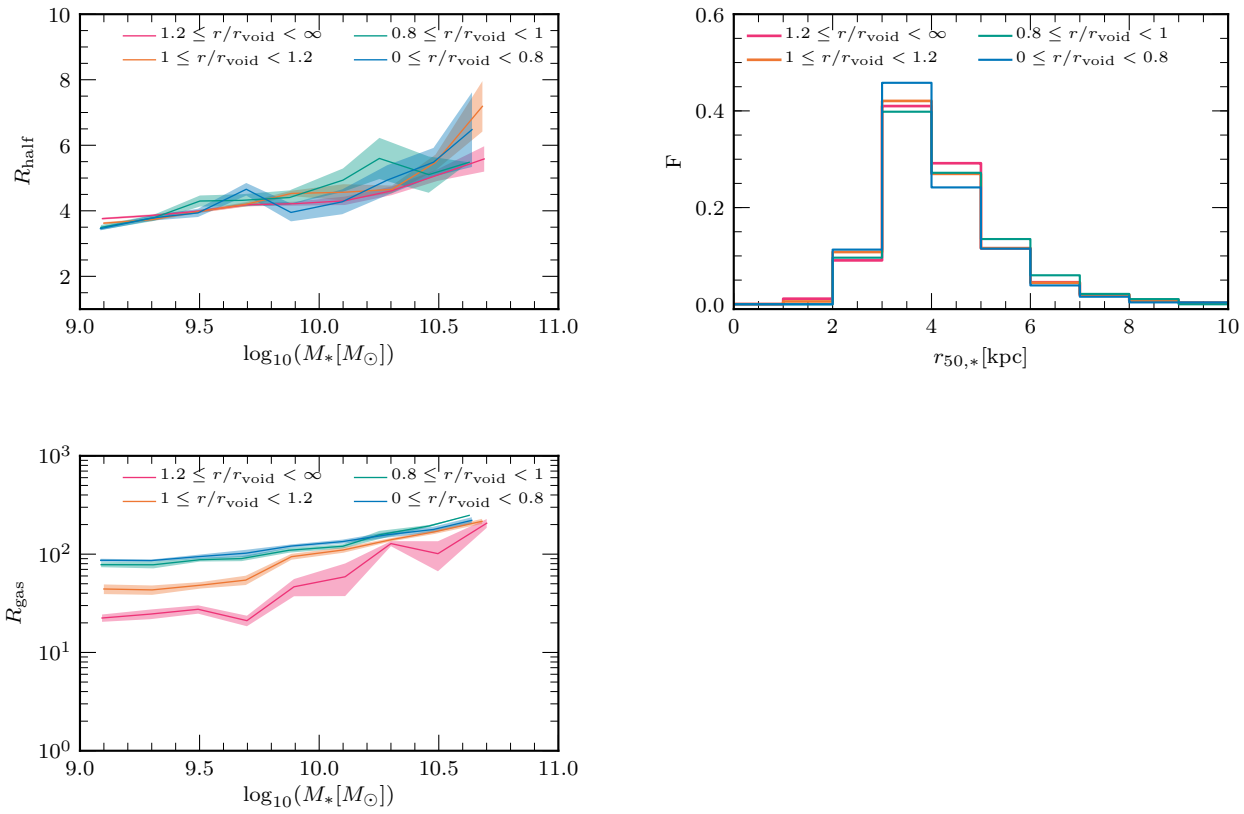

Figure 11. Distributions of the galaxy sizes for the different samples. We did not find a visible difference between different galaxy samples. Calculating the KS test we find that there is no differences between distributions (p-value > 0.12).